Characterization of Two VQIXXK Motifs for Tau Fibrillization *in Vitro*†

Wenkai Li‡,§ and Virginia M.-Y. Lee*,‡

Center for Neurodegenerative Disease Research, Department of Pathology and Laboratory Medicine, and Department of Biochemistry and Molecular Biophysics, University of Pennsylvania School of Medicine, Philadelphia, Pennsylvania 19104

Received July 14, 2006; Revised Manuscript Received October 31, 2006

ABSTRACT: Tau proteins are building blocks of the filaments that form neurofibrillary tangles of Alzheimer's disease (AD) and related neurodegenerative tauopathies. It was recently reported that two VQIXXK motifs in the microtubule (MT) binding region, named PHF6 and PHF6*, are responsible for tau fibrillization. However, the exact role each of these motifs plays in this process has not been analyzed in detail. Using a recombinant human tau fragment containing only the four MT-binding repeats (K18), we show that deletion of either PHF6 or PHF6* affected tau assembly but only PHF6 is essential for filament formation, suggesting a critical role of this motif. To determine the amino acid residues within PHF6 that are required for tau fibrillization, a series of deletion and mutation constructs targeting this motif were generated. Deletion of VQI in either PHF6 or PHF6* lessened but did not eliminate K18 fibrillization. However, removal of the single K^{311} residue from PHF6 completely abrogated the fibril formation of K18. K311D mutation of K18 inhibited tau filament formation, while K311A and K311R mutations had no effect. These data imply that charge change at position 311 is important in tau fibril formation. A similar requirement of nonnegative charge at this position for fibrillization was observed with the full-length human tau isoform (T40), and data from these studies indicate that the formation of fibrils by T40K311D and T40K311P mutants is repressed at the nucleation phase. These findings provide important insights into the mechanisms of tau fibrillization and suggest targets for AD drug discovery to ameliorate neurodegeneration mediated by filamentous tau pathologies.

Tau is a family of microtubule (MT)[1] associated proteins that promote the stability of the cytoskeleton through interactions with MTs (*1*−*3*). Neurofibrillary tangles (NFTs) consisting of pathological tau filaments are hallmark lesions of Alzheimer's disease (AD) and related neurodegenerative tauopathies such as corticobasal degeneration, progressive supranuclear palsy, Pick's disease, and frontotemporal dementia and parkinsonism linked to chromosome 17 (FTDP-17) (*3*). NFTs are composed of paired helical filaments (PHFs) or straight filaments assembled from abnormal tau and accumulate in neurons and glia (*3*, *4*). Since tau pathologies are mechanistically linked to a large number of age-related neurodegenerative diseases, they are potential targets for the development of therapeutic interventions.

Initial insights into the sequence requirements for tau fibrillization came from studies of PHFs derived from the AD brain that led to the identification of a pronase-resistant core in tau filaments consisting of the highly conserved MT-binding domain of all six tau isoforms (*5*−*8*). This implied that the region in tau containing either three or four alternatively spliced MT-binding repeats (i.e., 3R or 4R tau) is the integral core element of pathological tau filaments.

Modeling tau fibrillization *in vitro* encountered difficulties initially but is now possible (*9*). Studies of tau fibrillization using recombinant full-length human 3R tau and tau fragments containing the MT-binding repeats have provided compelling evidence for the essential role of the positively charged MT-binding repeat region in tau fibrillization (*10*−*12*). Significantly, sulfated glycosaminoglycans, heparin (*13*, *14*), and other polyanion cofactors such as RNA (*15*, *16*) and arachidonic acid (*17*, *18*) were shown to induce or accelerate tau polymerization into fibrils with properties characteristic of amyloid. Thus, the identification of conditions for *in vitro* assembly of tau into PHFs has paved the way for elucidating the molecular mechanism of tau amyloidogenesis.

A recent report suggests that two small fragments of the tau MT-binding repeat region, ^{265}KVQIINKK^{272} at the beginning of the second MT repeat and ^{247}VRSKIGSTENLKHQPGGGKVQIINKK^{272} spanning the first and second MT repeat, also produce AD-like tau filaments (*19*). More recently, it has been shown that two VQIXXK motifs in the second (R2) and third (R3) MT-binding repeats of tau, ^{275}VQIINK^{280} (PHF6* in R2) and ^{306}VQIVYK^{311} (PHF6 in R3), are important for β-sheet structure development and the initiation of tau fibril formation (*9*, *20*, *21*). However, the

† This work was supported by grants from the National Institute on Aging. V.M.-Y.L. is the John H. Ware III Professor for Alzheimer's Research.

* Address correspondence to this author. Tel: 215-662-6427. Fax: 215-349-5909. E-mail: vmylee@mail.med.upenn.edu.

‡ Center for Neurodegenerative Disease Research, Department of Pathology and Laboratory Medicine, University of Pennsylvania School of Medicine.

§ Department of Biochemistry and Molecular Biophysics, University of Pennsylvania School of Medicine.

[1] Abbreviations: AD, Alzheimer's disease; MT, microtubule; NFTs, neurofibrillary tangles; FTDP-17, frontotemporal dementia and Parkinsonism linked to chromosome 17; PHFs, paired helical filaments; WT, wild type; ThT, thioflavin T; PMSF, phenylmethylsulfonyl fluoride; SDS−PAGE, sodium dodecyl sulfate−polyacrylamide gel electrophoresis; EM, electron microscopy; Aβ, amyloid β peptide.

10.1021/bi061422+ CCC: $33.50
Published on Web 12/19/2006

functional differences between PHF6 and PHF6* remain unclear.

Here we show that deletion of either PHF6 or PHF6* affected the assembly of the human K18 tau construct, but only the absence of the former made K18 incompetent for fibrillization. Further mutagenesis studies of the PHF6 motif in K18 indicated that a positively or neutrally charged residue at 311 is required for the nucleation and fibrillization of tau.

MATERIALS AND METHODS

Chemicals. Low molecular weight heparin sodium salt (MW ≈ 5000 Da) was purchased from MP Biomedicals, LLC (Aurora, OH). The amyloid-binding dye thioflavine T (ThT) was obtained from Sigma (St. Louis, MO).

Cloning, Expression, and Purification of Proteins. The longest wild-type (WT) human tau isoform (T40) with 441 amino acid residues and tau fragments consisting of the MT-binding region of WT 4R tau (K18) (starting from Q244 and ending with E372 and numbering of the amino acid sequences is according to T40) (Figure 1A) were cloned into the *Nde*I and *Eco*RI restriction sites of the bacterial expression vector pRK172. The cDNAs coding for the mutant tau proteins K18ΔPHF6, K18ΔPHF6*, K18ΔPHF6&6*, K18Δ7R4, K18ΔPHF3, K18ΔPHF3*, K18ΔK280, K18ΔK311, K18ΔK280&K281 (ΔKK), K18K280P, K18K311P, K18K311A, K18K311D, K18K311R, T40K311A, T40K311D, T40K311R, T40K311P, and T40ΔK311 (see Figure 1A) were engineered by creating the corresponding nucleotide substitutions and deletions in the WT cDNA using complementary sets of synthetic single-stranded primers bearing the mutant sequence and the QuikChange site-directed mutagenesis kit (Stratagene, La Jolla, CA). The correct reading frames of all of the plasmids were confirmed by DNA sequencing. The proteins were expressed in *Escherichia coli* BL21(DE3) RIL strain. Bacteria were grown in TB media containing ampicillin at 37 °C and induced with isopropyl-β-D-thiogalactopyranoside at a final concentration of 0.8 mM when the OD reached 0.6. After agitation for 2 h, cells were harvested by centrifugation. The pellet was resuspended in high-salt RAB buffer [0.1 M MES, 1 mM EGTA, 0.5 mM $MgSO_4$, 0.75 M NaCl, 0.02 M NaF, 1 mM phenylmethylsulfonyl fluoride (PMSF), 0.1% protease inhibitor cocktail (100 μg/mL each of pepstatin A, leupeptin, TPCK, TLCK, and soybean trypsin inhibitor and 100 mM EDTA), pH 7.0] and homogenized. The cell lysates were heated to 100 °C for 10 min, rapidly cooled on ice for 20 min and centrifuged at 70000*g* for 30 min. Supernatants were dialyzed into FPLC buffer A [20 mM piperazine-*N*,*N*′-bis(2-ethanesulfonic acid), 10 mM NaCl, 1 mM EGTA, 1 mM $MgSO_4$, 2 mM DTT, 0.1 mM PMSF, pH 6.5], applied onto a HiTrap Sepharose HP IEX cation-exchange column (Amersham Pharmacia Biotech, Inc., Piscataway, NJ), and eluted with a 0−0.4 M NaCl gradient using an ÄKTA basic FPLC system (Amersham Pharmacia Biotech, Inc., Piscataway, NJ). The fractions were checked for the presence of the tau proteins by sodium dodecyl sulfate−polyacrylamide gel electrophoresis (SDS−PAGE) followed by Coomassie Blue R-250 staining. Those containing the desired tau profile were pooled together and dialyzed against 100 mM sodium acetate buffer, pH 7.0. Proteins were concentrated using an Amicon YM-10 centrifuge concentrator (Millipore Corp., Bedford, MA). Protein concentrations were determined using the

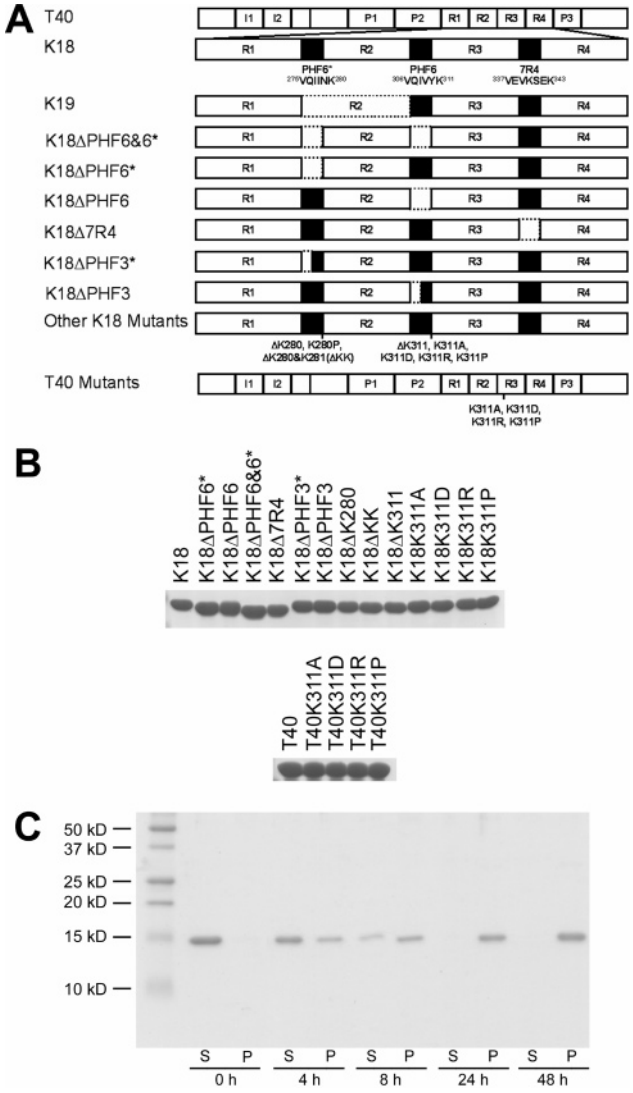

FIGURE 1: Human tau isoforms, mutants, and constructs. (A) Diagram of human tau isoforms, mutants, and constructs. The top bar shows the longest tau isoform tau40 (441 amino acids) in the CNS. The C-terminal half of tau contains three or four pseudorepeats (~31 residues each, R1−R4) together with their proline-rich flanking regions (P) that constitute the MT-binding domain. Repeat R2 and the two near N-terminal inserts (I1 and I2) may be absent due to alternative splicing. Two VQIXXK motifs, i.e., ^{275}VQIINK^{280} (designated as PHF6*) and ^{306}VQIVYK^{311} (designated as PHF6), at the beginning of R2 and R3 (solid) are reported to be important for PHF formation because they induce β-sheet structure. The corresponding N-terminal segment of the fourth repeat region 7R4 (^{337}VQIINK^{343}, solid) is predicted to possess β-sheet-forming potential. The first three amino acids (i.e., VQI) of PHF6* and PHF6 are named PHF3* and PHF3, respectively. Construct K18 comprises only four repeats (R1−R4), and construct K19 comprises only three repeats (R1, R3, and R4). The mutant ΔK^{280} occurs in FTDP-17. K^{280} and the corresponding Lys residue in R3, K^{311}, were deleted or mutated to Ala, Asp, Arg, and Pro. Since the residue following K^{280} is another Lys, K^{281}, a construct with both Lys residues deleted was also generated. K^{311} in T40 was also mutated to Ala, Asp, Arg, and Pro. (B) Coomassie Blue R-250-stained SDS−polyacrylamide gel of purified human recombinant tau proteins. Five hundred ng of each protein was loaded on the gel. (C) A representative Coomassie Blue R-250-stained SDS−polyacrylamide gel for sedimentation analysis of K18 fibrillization. K18 was assembled at a concentration of 20 μM in 100 mM sodium acetate, pH 7.0, 50 μM heparin, 2 mM DTT, and 0.04% sodium azide at 37 °C for 48 h by continuous shaking at 1000 rpm. S and P represent supernatant and pellet, respectively.

bicinchoninic acid protein assay (Pierce, Rockford, IL) with bovine serum albumin as a standard.

Filament Assembly. Filament assembly was started by making a master mix of 20 μM tau protein in 100 mM sodium acetate, pH 7.0, in the presence of 2 mM DTT and 0.04% sodium azide. After heat treatment at 55 °C for 10 min, a final concentration of 50 μM low molecular weight heparin was added to induce the assembly, and samples were dispensed immediately into PCR tubes followed by shaking on a tabletop Eppendorf Thermomixer R at 37 °C at 1000 rpm. The progress of aggregation was monitored by ThT fluorescence assay and electron microscopy (EM). Experiments were repeated with at least two different batches of purified proteins.

Thioflavine T (ThT) Fluorescence Assay. At each time point, 10 μL of each sample was taken out and loaded onto a 96-well plate for fluorometric reading. ThT (90 μL) diluted in 100 mM glycine buffer (pH 8.5) was added to the samples such that the final concentration of ThT was 5 μM. The excitation wavelength and emission wavelength of the fluorometer were set to 450 and 510 nm, respectively.

Sedimentation Analysis. Samples left after fluorometric assay were centrifuged at 100000*g* for 30 min to generate a pellet fraction containing fibrils and a supernatant containing unassembled tau protein. SDS sample buffer (10 mM Tris, pH 6.8, 1 mM EDTA, 40 mM DTT, 1% SDS, 10% sucrose) was added to pellets and supernatants, which were heated to 100 °C for 5 min. The samples were run on SDS−PAGE gels containing 10% or 15% polyacrylamide (*22*), and the percentages of tau protein in the supernatants and pellets were quantified by densitometry of the Coomassie Blue R-250-stained gels using ImageQuant 5.0.

Negative Staining EM. Negative staining EM was performed to confirm filament assembly and examine the morphology of tau fibrils and their structural intermediates. Briefly, 5 μL of the resuspended pellet was placed on 300 mesh carbon-coated copper/nickel grids for 5 min, washed five times with phosphate-buffered saline for 5 min each, stained with 2% uranyl acetate, and visualized with a Joel 1010 transmission electron microscope (Peabody, MA). Images were captured with a Hamamatsu digital camera (Bridgewater, MA) using AMT software (Danvers, MA).

Size Exclusion Chromatography. To determine whether oligomers were formed by T40 and T40K311 mutants, size exclusion chromatography was performed on an ÄKTA basic FPLC system (Amersham Pharmacia Biotech, Inc., Piscataway, NJ). About 300 μg of tau protein that had been assembled at 37 °C for 15 days was loaded onto a Superose 6 column and eluted with 100 mM sodium acetate buffer containing 2 mM DTT (pH 7.0) at a flow rate of 0.5 mL/min. For T40, T40K311A, and T40K311R, the samples were centrifuged for 2 min at 12000 rpm with a tabletop centrifuge to remove the filaments but not the oligomers before being loaded. The chromatography fractions were checked for the presence of tau proteins by SDS−PAGE, and the gel was either silver stained with the SilverQuest silver staining kit from Invitrogen (Calsbad, CA) or stained with Coomassie Blue R-250.

TANGO Calculation. TANGO, a computer algorithm for prediction of aggregating regions in unfolded polypeptide chains, can be accessed on the worldwide web at http://tango.embl.de/. Default parameters and conditions were used for calculation, i.e., pH = 7, temperature = 298.15 K, ionic strength = 0.02 M, TFE concentration = 0, and protein stability = −10 kcal/mol.

RESULTS

PHF6 but Not PHF6 Is Required for Tau Fibril Formation.* Previous studies have shown that two VQIXXK motifs, PHF6* and PHF6 at the N-termini of the second (R2) and the third repeat (R3) of the MT-binding domain of tau (K18), promote tau polymerization with their relatively high potential of adopting β-sheet structure (*20*, *21*) (Figure 1A). Additionally, secondary structure prediction of tau protein indicates that the beginning of the fourth repeat (R4), designated as 7R4, might also form β-structure though the sequence is quite different from PHF6* and PHF6 (Figure 1A). To determine the contributions of each of these N-terminal tau MT repeat sequences, i.e., PHF6*, PHF6, and 7R4, to tau fibrillization, we deleted these sequences singly or in combination (see Figure 1A) and generated recombinant WT and mutant tau proteins in *E. coli*. Purified recombinant tau proteins (Figure 1B) were incubated in the presence of heparin for different lengths of time, and the extent to which tau fibrils were formed was determined by (1) fluorometric assays to quantify the amount of β-pleated sheet structures, (2) sedimentation analysis to monitor the amount of fibrils that is pelletable (Figure 1C), and (3) negative staining EM to verify the formation of straight filaments and/or PHFs. Using these methods, we show that deletion of both hexapeptide motifs (PHF6* and PHF6) in K18 rendered the mutant K18ΔPHF6&6* unable to form tau filaments (Figure 2), supporting previous claims that PHF6* and PHF6 are important for tau fibrillization (*20*, *21*). To determine if both or only one of them is required for tau fibrillization, PHF6* and PHF6 were individually deleted from R2 and R3 to generate K18ΔPHF6* and K18ΔPHF6 mutants. The filament formation assay showed that polymerization of K18ΔPHF6* was significantly decreased but not abolished. On the other hand, K18ΔPHF6 failed to fibrillize (Figure 2A). These results suggest that PHF6 is vital for tau fibril formation while PHF6* is not. However, PHF6* does facilitate this process. These ThT fluorescence assay results were confirmed by sedimentation analysis and EM (Figure 2B,C).

Since the seven amino acids at the beginning of the fourth repeat are predicted to give rise to β-sheet structure (*23*), we hypothesized that they might also contribute to tau fibrillization in a mode similar to PHF6 and PHF6*. To address this issue, we deleted these residues and generated the K18Δ7R4 tau fragment. Unexpectedly, the fibrillization of this K18 mutant was not reduced but instead greatly accelerated (Figure 2A), suggesting that this motif impedes the fibrillization process. The enhanced fibril formation of the K18Δ7R4 mutant was verified by sedimentation analysis and EM (Figure 2B). After 24 h incubation, K18, K18ΔPHF6*, and K18Δ7R4 all formed straight filaments and PHF-like structures similar in morphology to those produced with T40 and authentic PHFs isolated from AD brains (Figure 2C) (*24*). Although incubation of K18ΔPHF6 failed to show a detectable ThT fluorescence signal (Figure 2A), rare globular structures and short filaments were seen by EM, suggesting that K18ΔPHF6 may be sufficient to drive nucleation but not elongation (Figure 2C). By contrast, similar incipient

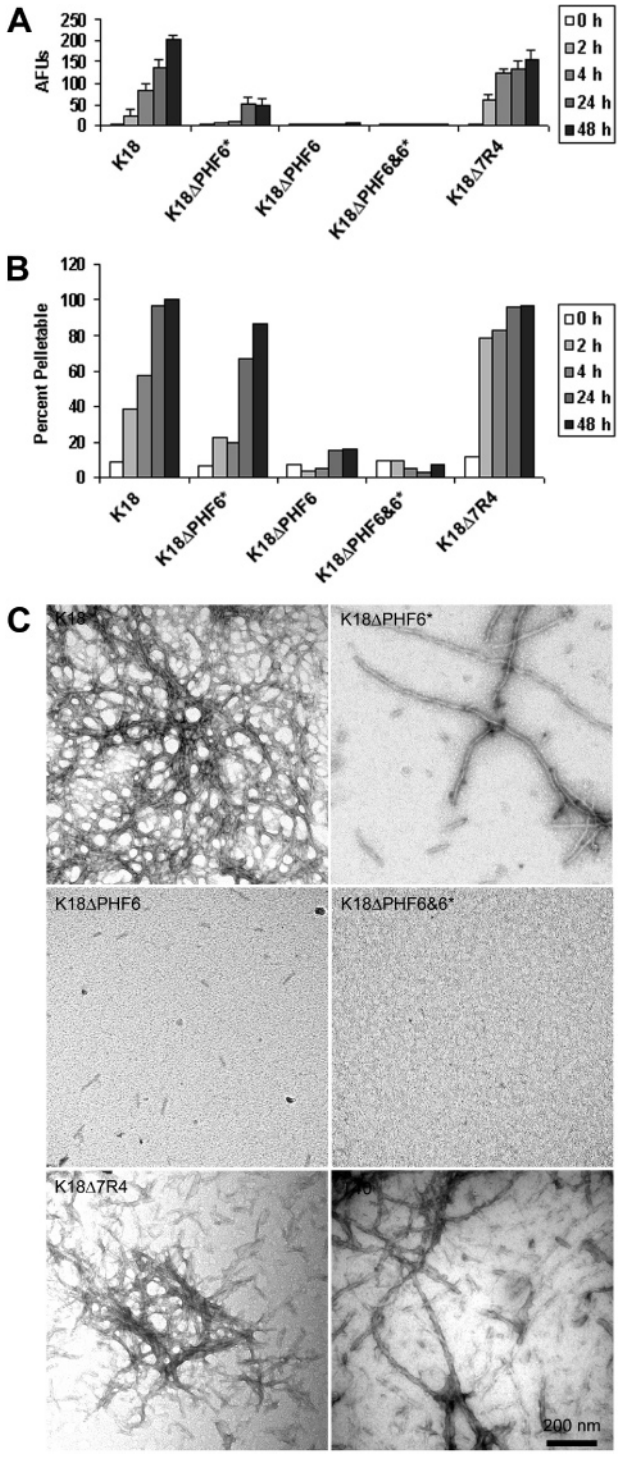

FIGURE 2: Filament assembly of K18, K18ΔPHF6*, K18ΔPHF6, K18ΔPHF6&6*, and K18Δ7R4. (A) ThT fluorescence assay of the filament assembly of K18, K18ΔPHF6*, K18ΔPHF6, K18ΔPHF6&6*, and K18Δ7R4. Conditions for filament assembly are described under Materials and Methods. AFUs, arbitrary fluorescence units. Error bars represent SD; $n = 3$. (B) Sedimentation analysis of the filament assembly of K18, K18ΔPHF6*, K18ΔPHF6, K18ΔPHF6&6*, and K18Δ7R4 in (A). Tau proteins in the supernatants and pellets were quantified by densitometry of the Coomassie Blue-stained gels. One of two representative gels was used for quantification. (C) Negative staining EM of the 24 h samples of K18, K18ΔPHF6*, K18ΔPHF6, K18ΔPHF6&6*, and K18Δ7R4 assembled in (A). For comparison, PHFs formed by T40 after 15 days are also shown. Procedures of EM study are described under Materials and Methods.

spherical structures were not detected with the double deletion mutant K18ΔPHF6&6* (Figure 2C).

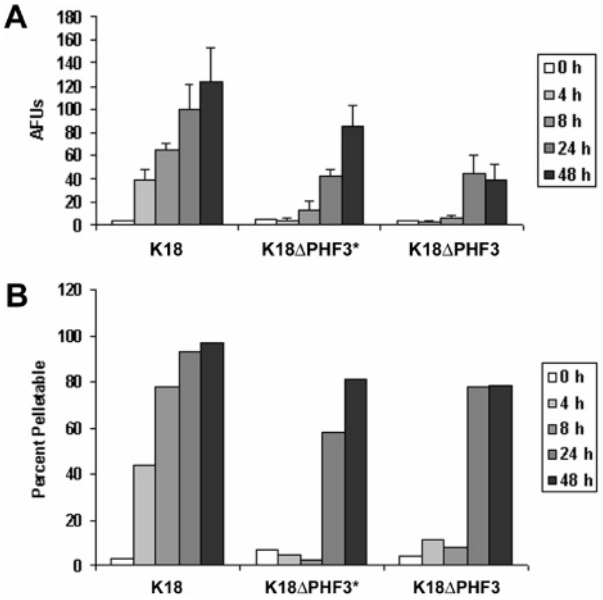

FIGURE 3: Filament assembly of K18, K18ΔPHF3*, and K18ΔPHF3. (A) ThT fluorescence assay of the filament assembly of K18, K18ΔPHF3*, and K18ΔPHF3. AFUs, arbitrary fluorescence units. Error bars represent SD; $n = 3$. (B) Sedimentation analysis of the filament assembly of K18, K18ΔPHF3*, and K18ΔPHF3 in (A). One of two representative gels was used for quantification.

The Conserved VQI Motifs in PHF6 and PHF6 Are Not Essential for Tau Fibrillization.* To determine if the conserved amino acid residues VQI of the VQIXXK motifs in PHF6 and PHF6* are required for tau fibrillization, VQI tau deletion mutants K18ΔPHF3* and K18ΔPHF3 were generated (Figure 1A,B). Compared to K18ΔPHF3*, the fibrillization of K18ΔPHF3 appeared to be more attenuated. However, the fibril assembly of neither K18ΔPHF3* nor K18ΔPHF3 was abolished (Figure 3A). Sedimentation analysis further supported the data from fluorometric assay (Figure 3B). Despite the slower rate of fibrillization, the appearance of filaments formed by these tau mutants, as examined by EM, was similar to that of WT K18 fibrils (data not shown).

The Role of C-Terminal Lysines in PHF6 and PHF6 of K18 for Fibrillization.* Since both PHF6 and PHF6* contain a conserved lysine residue at the C-terminus, we examined the effects of deleting this amino acid residue from either PHF6* (ΔK280) or PHF6 (ΔK311) on K18 fibril formation. Previous studies have identified ΔK280 as an autosomal dominantly inherited FTDP-17 tau gene mutation (*25*, *26*), and recent studies suggest that recombinant ΔK280 mutant tau polymerizes *in vitro* more readily than its WT counterpart in the presence of heparin (*27*). Similar to these previous studies, we found that K18ΔK280 fibrillized much faster than K18. The assembly of K18ΔK280 reached a plateau after 4 h while only 20% of K18 was fibrillized (Figure 4A). On the other hand, K18ΔK311 was unable to form fibrils even after 48 h of incubation (Figure 4A). Similar results were also obtained when K^{311} was substituted by proline, a β-sheet breaker. But K18K280P continued to fibrillize albeit at a much slower rate than K18 and K18Δ280 (Figure 4B).

Since another lysine normally occurs at residue 281 in human tau, removal of either K^{280} or K^{281} would keep the VQIXXK motif intact. For this reason, we examined the effect of eliminating both lysine residues simultaneously on

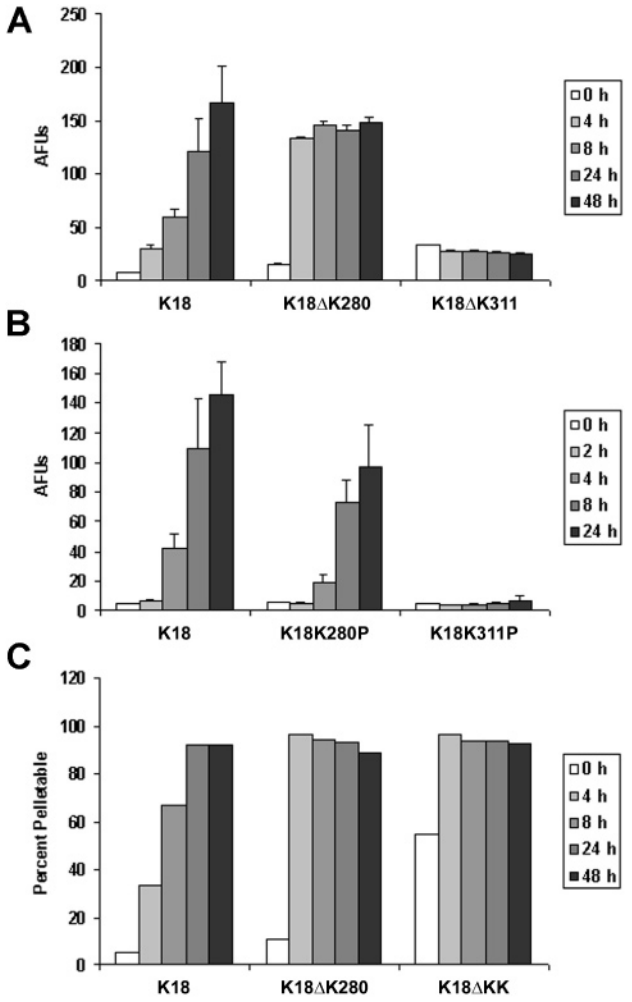

FIGURE 4: Role of Lys in PHF6 and PHF6* in tau filament assembly. (A) ThT fluorescence assay of the filament assembly of K18, K18ΔK280, and K18ΔK311. AFUs, arbitrary fluorescence units. Error bars represent SD; $n = 3$. (B) ThT fluorescence assay of the filament assembly of K18, K18K280P, and K18K311P. AFUs, arbitrary fluorescence units. Error bars represent SD; $n = 3$. (C) Sedimentation analysis of the filament assembly of K18, K18ΔK280, and K18ΔKK. One of two representative gels was used for quantification.

tau fibrillization. Sedimentation analysis conducted with K18, K18ΔK280, and K18ΔKK (i.e., ΔK280 and ΔK281) showed that the double deletion mutant K18ΔKK assembled even faster than K18ΔK280. Indeed, significant amounts of tau filaments appeared immediately after heparin was added (Figure 4C) with maximum fibril numbers achieved in less than 4 h (data not shown) while K18ΔK280 and K18 produced very few fibrils at this early time. Representative EM images of each K18 mutant construct after assembly for 24 h show that the morphology of the filaments is quite similar to that of K18 filaments illustrated in Figure 2C (data not shown). Consistent with the inability of K18ΔK311 to form fibrils (Figure 4A), no oligomers or filaments were detected by EM. Thus, while K^{280} and/or K^{281} in PHF6* are dispensable for K18 fibrillization, K^{311} in PHF6 is essential, suggesting different roles of C-terminal lysine residues of PHF6* and PHF6 in mediating K18 tau fibril formation.

To further investigate the role of K^{311} in K18 fibrillization, we generated a series of point mutations replacing this lysine with either negatively charged (K311D), neutral (K311A), or positively charged (K311R) residues. Both K18K311A

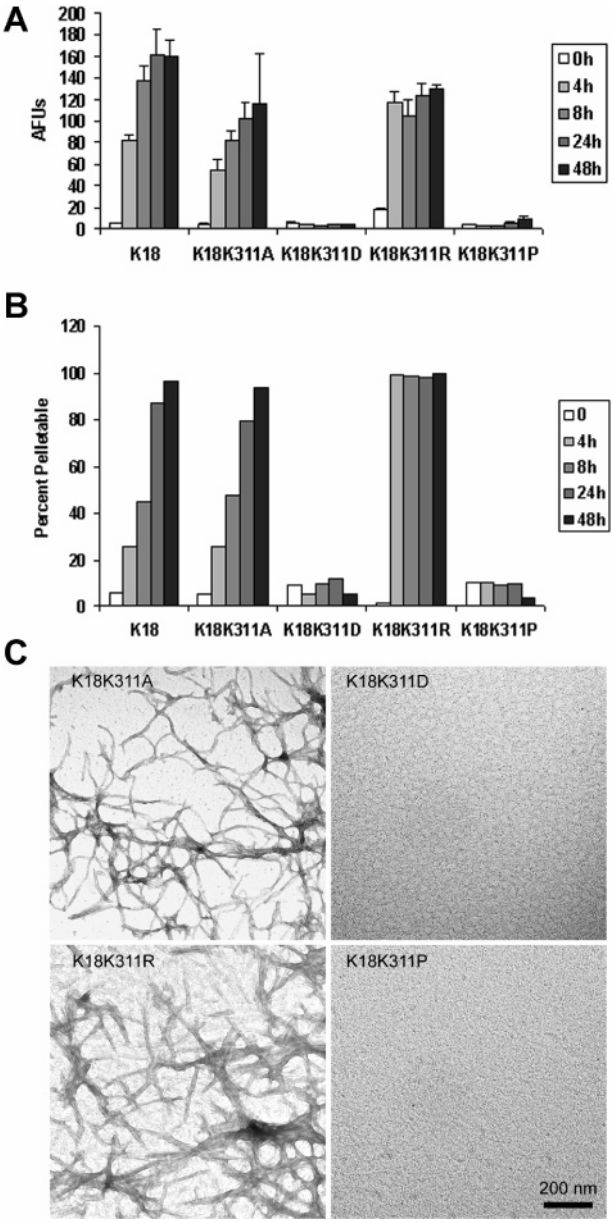

FIGURE 5: Filament assembly of K18, K18K311A, K18K311D, K18K311R, and K18K311P. (A) ThT fluorescence assay of the filament assembly of K18, K18K311A, K18K311D, K18K311R, and K18K311P. AFUs, arbitrary fluorescence units. Error bars represent SD; $n = 3$. (B) Sedimentation analysis of the filament assembly of K18, K18K311A, K18K311D, K18K311R, and K18K311P. One of two representative gels was used for quantification. (C) Negative staining EM of the 24 h samples of K18K311A, K18K311D, K18K311R, and K18K311P assembled in (A).

and K18K311R retained the ability to form fibrils with the latter fibrillizing even faster than K18 in both ThT assays and sedimentation analyses (Figure 5A,B). However, the fibrillization was completely abolished with the introduction of a negatively charged residue at K^{311} in the mutant of K18K311D (Figure 5A,B). EM studies indicated that the morphology of the fibrils formed by K18 (Figure 2C), K18K311A, and K18K311R (Figure 5C) were analogous whereas K18K311D and K18K311P did not even form oligomers or short filaments (Figure 5C). These findings with K18 mutants suggest that the charge at position 311 is important for the initiation of tau fibrillization.

Similar K^{311} mutations were introduced into the largest full-length human tau isoform (T40), and the recombinant

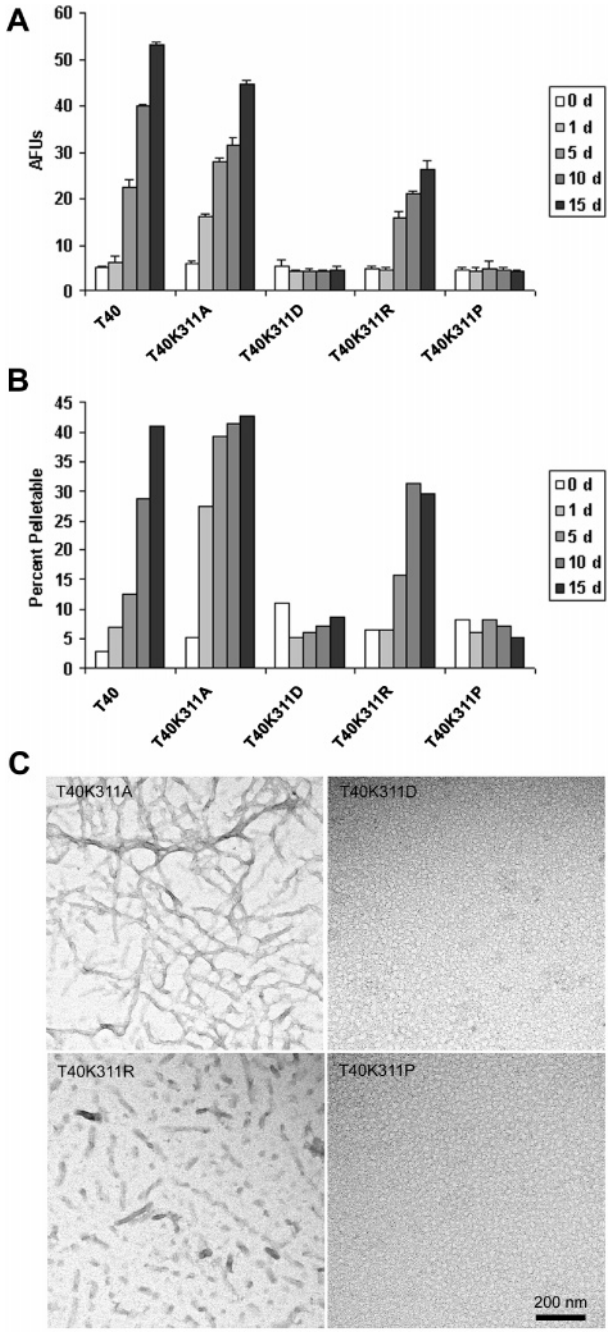

FIGURE 6: Filament assembly of T40, T40K311A, T40K311D, T40K311R, and T40K311P. (A) ThT fluorescence assay of the filament assembly of T40, T40K311A, T40K311D, T40K311R, and T40K311P. AFUs, arbitrary fluorescence units. Error bars represent SD; $n = 3$. (B) Sedimentation analysis of the filament assembly of T40, T40K311A, T40K311D, T40K311R, and T40K311P. One of two representative gels was used for quantification. (C) Negative staining EM of the 24 h samples of T40K311A, T40K311D, T40K311R, and T40K311P assembled in (A).

proteins were expressed and purified for tau fibrillization assays. Due to the slow kinetics of T40 fribrillization, the assay was performed for up to 15 days. Consistent with the assembly properties of K18K311 mutants described above, T40K311A and T40K311R retained the ability to fibrillize as monitored by both ThT assay (Figure 6A) and sedimentation analysis (Figure 6B). T40K311A fibrillized faster than T40 at earlier time points, but T40K311R assembled into fibrils at a slower rate. The flanking sequences N- and C-terminal to the MT-binding repeat region of K18 in T40 probably contribute to these slightly different behaviors. As expected, T40K311D, T40K311P, and T40ΔK311 could not fibrillize (Figure 6A,B and Supporting Information, Figure 1B), and the lack of tau oligomers and filaments was further demonstrated by EM (Figure 6C and Supporting Information, Figure 1C).

The background level fluorescence reading and the nonexistence of oligomers and short fibrils in the assembly of T40K311D and T40K311P suggest that their fibrillization fails at the nucleation phase rather than the elongation phase. To further confirm the abrogation of nucleation, we performed size exclusion chromatography on wild-type and mutant samples after 15-day assembly. As predicted, the chromatograms of T40, T40K311A, and T40K311R showed two major peaks, a large peak eluted earlier followed by a smaller peak (Figure 7A,B,D). SDS−PAGE showed that both peaks were tau, and under nonreducing conditions, the large peak migrated partially as high molecular weight species but not the small one (Figure 7F). Apparently, the first one is an oligomer peak, and the second one is a monomer peak. The monomeric nature of the second peak was also verified by comparing with the trace of unassembled T40 on our size exclusion chromatography (data not shown). In contrast, the chromatogram of T40K311D and T40K311P showed the presence of only a single peak at the same elution volume as T40 monomers (Figure 7C,E). Thus, our gel filtration data are consistent with the results from ThT assays and EM analyses that T40K311D and T40K311P are unable to nucleate for fibril formation.

DISCUSSION

Tau is a highly soluble protein that does not possess any significant secondary structures in the normal state (*2*, *28*). Although the role of tau aggregates in AD and the other related neurodegenerative diseases is still a matter of debate, accumulating evidence implicates these tau lesions in the onset and/or progression of tauopathies (*29*−*31*). As a result, therapeutic strategies are being pursued to inhibit tau fibrillization or to dissolve filamentous tau lesions (*32*−*35*). The major structural elements of tau tangles are PHFs and straight filaments (*4*, *36*). The key part of tau protein for fibril formation lies in its MT-binding repeat region, which fibrillizes more readily than the full-length molecule in *in vitro* assays (*8*, *10*, *37*−*39*). Furthermore, two VQIXXK motifs within R2 and R3 have been proposed to be critical for tau fibrillization through the initial formation of β-structure in this natively unfolded protein (*9*, *20*, *21*).

The first question we addressed was whether or not the N-terminal sequences of R2, R3, and R4 were essential for tau fibrillization. Using K18 and T40 constructs, we showed that only deletion of PHF6 within R3 abolished tau fibrillization, suggesting that this amino acid stretch is essential for tau to assemble into pathological filaments, while removing the PHF6* motif within R2 reduced the kinetics of this process. Thus, contrary to the previous report (*21*), tau fibrillization does not require participation of both VQIXXK motifs. In fact, it has been demonstrated that although R2 can enhance tau fibrillization, it is not required (*10*−*12*) even though PHFs are highly abundant in neurodegenerative tauopathy brains where four-repeat tau isoforms predominate (*40*−*42*).

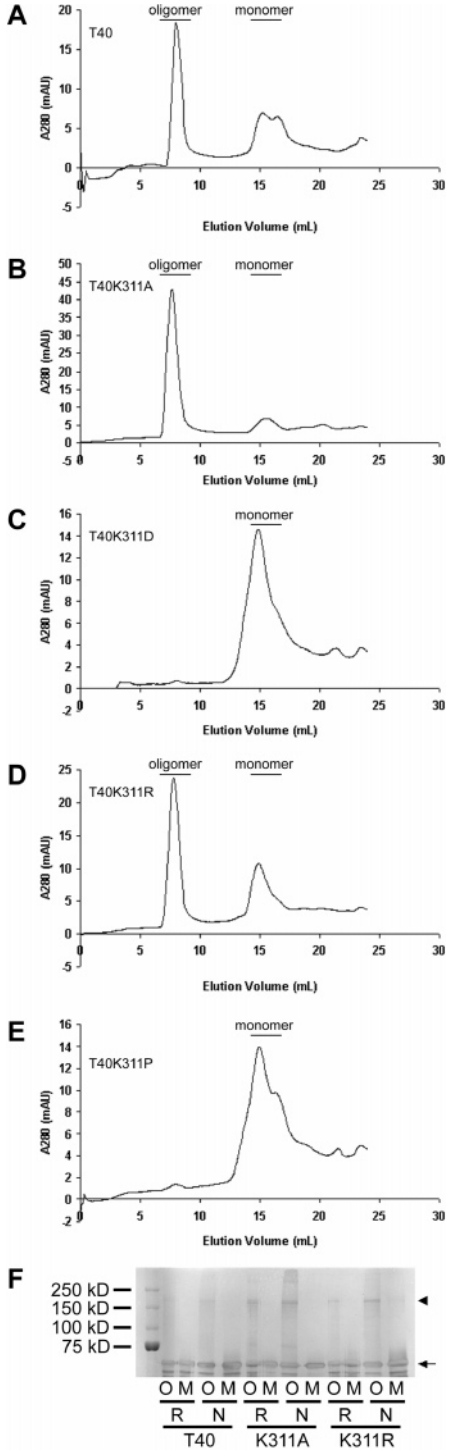

FIGURE 7: Size exclusion chromatography analysis of T40 (A), T40K311A (B), T40K311D (C), T40K311R (D), T40K311P (E). All samples were prepared as described under Materials and Methods. Samples were shaken at 37 °C for 15 days for assembly, and monomeric and oligomeric wild-type and mutant T40 were separated using a Superose 6 column and eluted with 100 mM sodium acetate buffer containing 2 mM DTT (pH 7.0). For T40, T40K311A, and T40K311R, the samples were centrifuged for 2 min at 12000 rpm with a tabletop centrifuge to remove the filaments. (F) SDS−PAGE analysis of the oligomer and monomer peaks of T40, T40K311A, and T40K311R. An 8% SDS−polyacrylamide gel was run with 20 μL samples loaded for each lane, and the gel was silver stained. Key: O, oligomer peak fraction; M, monomer peak fraction; R, reducing agent (DTT) in the SDS−PAGE sample buffer; N, no reducing agent in the SDS−PAGE sample buffer; K311A, T40K311A; K311R, T40K311R. The arrowhead denotes oligomeric tau, and the arrow points to monomeric tau.

The discovery that K18Δ7R4 fibrillizes more rapidly than K18 suggests that 7R4 may serve to prevent tau aggregation despite its location in the pronase-resistant PHF core region (*43*). Since glutamate is known to be a β-sheet breaker, the existence of two glutamate residues in 7R4 may explain its inhibitory effects on tau fibrillization. It is plausible that similar properties are associated with the equivalent region in R1 (^{244}QTAPVPM^{250}) because of the presence of another β-sheet breaker proline. Thus, while R2 and R3 probably are integral elements of tau fibrils, R1 and R4 may play modulatory roles in the tau fibrillization process (*20*). Indeed, a recent report demonstrated high self-aggregation abilities for R2 and R3 peptides but low self-aggregation abilities for R1 and R4 peptides (*44*). Since we observed that no fibrils were formed by the double deletion K18 mutant in which both PHF6 and PHF6* were absent and that the nucleation phase also was disrupted, these and other data presented here lead us to conclude that PHF6 is critical for the elongation of tau filaments, while either of the VQIXXK motifs may be sufficient for nucleation of tau fibrillization.

Interestingly, the shared sequence of VQI in both VQIXXK motifs is not essential for tau fibril formation. Moreover, fibrillization studies of a series of peptides derived from PHF6 suggest that the fibril core of PHF6 lies in the VYK region, and even the N-acetylated YK dipeptide forms large crystalline-like spherical and globular structures reminiscent of those formed by WT tau (*45*), while other studies imply that Y^{310} plays an essential role in tau fibrillization (*20*, *46*). Thus, it is reasonable to hypothesize that an aromatic residue at position 310 interacts with another aromatic residue of the neighboring monomer by π-stacking and stabilizing the association of β-sheet structures between tau molecules, as does Y^{181} in cytolysin during its oligomerization and intersubunit β-strand alignment (*47*). A most recent report on the structure of core tau sequences around the PHF6 region actually provides strongest support to our hypothesis (*48*). Accordingly, it will be important to determine if ^{278}INK^{280}, the three amino acids in PHF6* corresponding to ^{309}VYK^{311} in PHF6, represents the core of PHF6*.

The important role of K^{311} in PHF6 in tau fibrillization is in stark contrast to the inhibitory role of K^{280} in PHF6*. It has been recognized that several of the tau mutations linked to FTDP-17, e.g., ΔK280 and P301L, have a particularly marked effect in promoting tau aggregation (*3*, *21*, *27*, *49*−*53*). Similar to previous studies, we found that the deletion of K^{280} enhanced tau fibrillization. Moreover, a K^{280} and K^{281} double deletion mutant (i.e., K18ΔKK) fibrillized even faster. However, deletion of K^{311} had exactly the opposite effect and resulted in the inability of tau to fibrillize. Our data suggest the importance of K^{311} in mediating the part of PHF6 or ^{309}VYK^{311} in tau fibril formation.

We propose that the two VQIXXK motifs are significantly different in their ability to modulate tau fibrillization. While K^{280} and K^{281} play inhibitory roles in tau aggregation, K^{311} is required for tau to assemble into fibrils. The different roles of the lysine residues in tau fibril formation can be appreciated by examining the sequences around the lysine residues. Using TANGO, a statistical mechanics algorithm that correctly predicts sequence-dependent aggregation of 250 peptides and proteins including tau sequences (*54*), we tried to understand the potential roles of different Lys residues (Figure 8). In K18, only the region around PHF6 is calculated to possess

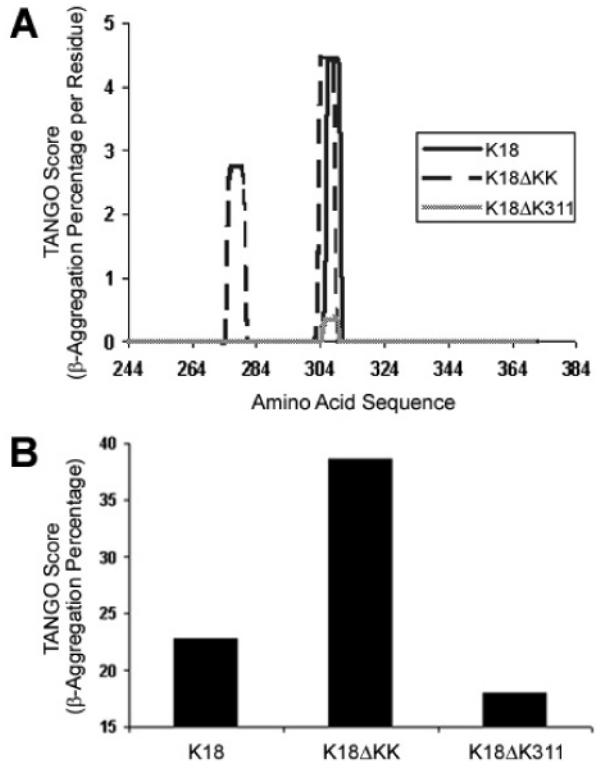

FIGURE 8: TANGO prediction of K18, K18ΔKK, and K18ΔK311 aggregation. (A) TANGO prediction of increased aggregation propensity of the PHF6* region in K18ΔKK and decreased aggregation propensity of the PHF6 region in K18ΔK311 in comparison with K18. (B) TANGO prediction of increased overall aggregation propensity of K18ΔKK and decreased overall aggregation propensity of K18ΔK311 in comparison with K18.

β-aggregation potential (Figure 8A). This is in agreement with our observation that only PHF6 is essential for tau filament formation (Figure 2). However, a second β-aggregation motif emerges around the PHF6* region when K^{280} and K^{281} are removed in K18ΔKK (Figure 8A). This may explain why K18ΔKK forms filaments more readily than K18. By contrast, the deletion of K^{311} in K18ΔK311 removed the only β-aggregation potential in PHF6, thereby producing a mutant incompetent for fibril formation (Figure 8A). Finally, the distinct assembly behavior of K18, K18ΔKK, and K18ΔK311 is reflected by the TANGO score for overall β-aggregation (Figure 8B). Thus, the abundant lysine residues (44 in T40) at different locations within tau protein probably serve intrinsically different functions.

Our mutagenesis studies of K^{311} also demonstrate the significance of charge at 311 since only positive or neutral substitutions facilitate tau fibrillization whereas substitution to a negative residue even completely eliminated the ability of tau to nucleate. Though hydrophobic interactions are well accepted as a driving force for β-sheet structure formation, some investigators have also pointed out the contribution of charge−charge interactions in this process. Selected substitution of charged residues in Aβ peptide, such as D23K, was shown to be able to avert its folding into a β-sheet conformation (*55*). The relationship between electrostatic charges and protein conformation seems far more complicated. Some determinants probably include the other residues within the sequence, the pH of the system, and the local environment of the charged residues.

The identification of PHF6 as an essential motif and K^{311} in PHF6 as the key residue for tau aggregation may offer new strategies in the development of potential therapeutics for neurodegenerative tauopathies. PHF6 peptide can specifically associate with full-length tau, probably through interaction with the PHF6 region (data not shown). It is possible that a modified PHF6 peptide, especially at the key K^{311} position, could inhibit tau fibrillization. For example, substitution with or inclusion of β-structure breakers such as proline and/or glutamate or utilization of stereochemically different D-amino acids could allow the peptide to retain its ability to bind to tau protein and stabilize its normal conformation, preventing misfolding, nucleation, and/or elongation of the protein. This approach has been adopted to reverse the formation of β-sheet-rich aggregated structure and deposition of β-amyloid and prion protein PrP plaques both *in vitro* and *in vivo* (*56*−*62*). For tau, this may be more difficult because the intracellular location makes it less accessible. Another strategy might be to modify the K^{311} residue of tau with small molecules to disrupt the function of PHF6 in tau aggregation either through the introduction of a β-structure breaking group or a negative charge, which can probably inhibit its assembly process just as the K311D mutation does. Here the biggest challenge is how to ensure the specificity of the modification, considering the existence of so many lysines in tau. With the progress in clarifying the principles governing tau aggregation, development of effective therapies to interfere with aggregation formation in tauopathies will become more efficient.

ACKNOWLEDGMENT

The authors thank Dr. John Trojanowski and Diana Shineman for critical reading of the manuscript. Chi Li is thanked for technical support on molecular cloning, and the Biochemical Imaging Core Facility of the University of Pennsylvania is thanked for assistance in the EM studies.

SUPPORTING INFORMATION AVAILABLE

Filament assembly of T40 and T40ΔK311 (Figure 1). This material is available free of charge via the Internet at http://pubs.acs.org.

REFERENCES

1. Weingarten, M. D., Lockwood, A. H., Hwo, S. Y., and Kirschner, M. W. (1975) A protein factor essential for microtubule assembly, *Proc. Natl. Acad. Sci. U.S.A. 72*, 1858−1862.
2. Cleveland, D. W., Hwo, S. Y., and Kirschner, M. W. (1977) Purification of tau, a microtubule-associated protein that induces assembly of microtubules from purified tubulin, *J. Mol. Biol. 116*, 207−225.
3. Lee, V., M.-Y., Goedert, M., and Trojanowski, J. Q. (2001) Neurodegenerative tauopathies, *Annu. Rev. Neurosci. 24*, 1121−1159.
4. Kidd, M. (1963) Paired helical filaments in electron microscopy of Alzheimer's disease, *Nature 197*, 192−194.
5. Wischik, C. M., Novak, M., Thogersen, H. C., Edwards, P. C., Runswick, M. J., Jakes, R., Walker, J. E., Milstein, C., Roth, M., and Klug, A. (1988) Isolation of a fragment of tau derived from the core of the paired helical filament of Alzheimer disease, *Proc. Natl. Acad. Sci. U.S.A. 85*, 4506−4510.
6. Crowther, R. A. (1991) Straight and paired helical filaments in Alzheimer disease have a common structural unit, *Proc. Natl. Acad. Sci. U.S.A. 88*, 2288−2292.

7. Novak, M., Kabat, J., and Wischik, C. M. (1993) Molecular characterization of the minimal protease resistant tau unit of the Alzheimer's disease paired helical filament, *EMBO J. 12*, 365−370.
8. Jakes, R., Novak, M., Davison, M., and Wischik, C. M. (1991) Identification of 3- and 4-repeat tau isoforms within the PHF in Alzheimer's disease, *EMBO J. 10*, 2725−2729.
9. Barghorn, S., and Mandelkow, E. (2002) Toward a unified scheme for the aggregation of tau into Alzheimer paired helical filaments, *Biochemistry 41*, 14885−14896.
10. Crowther, R. A., Olesen, O. F., Jakes, R., and Goedert, M. (1992) The microtubule binding repeats of tau protein assemble into filaments like those found in Alzheimer's disease, *FEBS Lett. 309*, 199−202.
11. Wille, H., Drewes, G., Biernat, J., Mandelkow, E. M., and Mandelkow, E. (1992) Alzheimer-like paired helical filaments and antiparallel dimers formed from microtubule-associated protein tau *in vitro*, *J. Cell Biol. 118*, 573−584.
12. Schweers, O., Mandelkow, E. M., Biernat, J., and Mandelkow, E. (1995) Oxidation of cysteine-322 in the repeat domain of microtubule-associated protein tau controls the in vitro assembly of paired helical filaments, *Proc. Natl. Acad. Sci. U.S.A. 92*, 8463−8467.
13. Goedert, M., Jakes, R., Spillantini, M. G., Hasegawa, M., Smith, M. J., and Crowther, R. A. (1996) Assembly of microtubule-associated protein tau into Alzheimer-like filaments induced by sulphated glycosaminoglycans, *Nature 383*, 550−553.
14. Perez, M., Valpuesta, J. M., Medina, M., Montejo, G., and Avila, J. (1996) Polymerization of tau into filaments in the presence of heparin: the minimal sequence required for tau−tau interaction, *J. Neurochem. 67*, 1183−1190.
15. Kampers, T., Friedhoff, P., Biernat, J., Mandelkow, E. M., and Mandelkow, E. (1996) RNA stimulates aggregation of microtubule-associated protein tau into Alzheimer-like paired helical filaments, *FEBS Lett. 399*, 344−349.
16. Hasegawa, M., Crowther, R. A., Jakes, R., and Goedert, M. (1997) Alzheimer-like changes in microtubule-associated protein Tau induced by sulfated glycosaminoglycans. Inhibition of microtubule binding, stimulation of phosphorylation, and filament assembly depend on the degree of sulfation, *J. Biol. Chem. 272*, 33118−33124.
17. Wilson, D. M., and Binder, L. I. (1997) Free fatty acids stimulate the polymerization of tau and amyloid beta peptides. In vitro evidence for a common effector of pathogenesis in Alzheimer's disease, *Am. J. Pathol. 150*, 2181−2195.
18. King, M. E., Ahuja, V., Binder, L. I., and Kuret, J. (1999) Ligand-dependent tau filament formation: implications for Alzheimer's disease progression, *Biochemistry 38*, 14851−14859.
19. Giannetti, A. M., Lindwall, G., Chau, M. F., Radeke, M. J., Feinstein, S. C., and Kohlstaedt, L. A. (2000) Fibers of tau fragments, but not full length tau, exhibit a cross beta-structure: implications for the formation of paired helical filaments, *Protein Sci. 9*, 2427−2435.
20. von Bergen, M., Friedhoff, P., Biernat, J., Heberle, J., Mandelkow, E. M., and Mandelkow, E. (2000) Assembly of tau protein into Alzheimer paired helical filaments depends on a local sequence motif ((306)VQIVYK(311)) forming beta structure, *Proc. Natl. Acad. Sci. U.S.A. 97*, 5129−5134.
21. von Bergen, M., Barghorn, S., Li, L., Marx, A., Biernat, J., Mandelkow, E. M., and Mandelkow, E. (2001) Mutations of tau protein in frontotemporal dementia promote aggregation of paired helical filaments by enhancing local beta-structure, *J. Biol. Chem. 276*, 48165−48174.
22. Laemmli, U. K. (1970) Cleavage of structural proteins during the assembly of the head of bacteriophage T4, *Nature 227*, 680−685.
23. Gamblin, T. C. (2005) Potential structure/function relationships of predicted secondary structural elements of tau, *Biochim. Biophys. Acta 1739*, 140−149.
24. Lee, V. M.-Y., Balin, B. J., Otvos, L., Jr., and Trojanowski, J. Q. (1991) A68: a major subunit of paired helical filaments and derivatized forms of normal Tau, *Science 251*, 675−678.
25. Rizzu, P., Van Swieten, J. C., Joosse, M., Hasegawa, M., Stevens, M., Tibben, A., Niermeijer, M. F., Hillebrand, M., Ravid, R., Oostra, B. A., Goedert. M., van Duijn, C. M., and Heutink, P. (1999) High prevalence of mutations in the microtubule-associated protein tau in a population study of frontotemporal dementia in the Netherlands, *Am. J. Hum. Genet. 64*, 414−421.
26. Hutton, M. (2000) Molecular genetics of chromosome 17 tauopathies, *Ann. N.Y. Acad. Sci. 920*, 63−73.
27. Barghorn, S., Zheng-Fischhöfer, Q., Ackmann, M., Biernat, J., von Bergen, M., Mandelkow, E. M., and Mandelkow, E. (2000) Structure, microtubule interactions, and paired helical filament aggregation by tau mutants of frontotemporal dementias, *Biochemistry 39*, 11714−11721.
28. Schweers, O., Schonbrunn-Hanebeck, E., Marx, A., and Mandelkow, E. (1994) Structural studies of tau protein and Alzheimer paired helical filaments show no evidence for beta-structure, *J. Biol. Chem. 269*, 24290−24297.
29. Wittmann, C. W., Wszolek, M. F., Shulman, J. M., Salvaterra, P. M., Lewis, J., Hutton, M., and Feany, M. B. (2001) Tauopathy in *Drosophila*: neurodegeneration without neurofibrillary tangles, *Science 293*, 711−714.
30. Kosik, K. S., and Shimura, H. (2005) Phosphorylated tau and the neurodegenerative foldopathies, *Biochim. Biophys. Acta 1739*, 298−310.
31. Feinstein, S. C., and Wilson, L. (2005) Inability of tau to properly regulate neuronal microtubule dynamics: a loss-of-function mechanism by which tau might mediate neuronal cell death, *Biochim. Biophys. Acta 1739*, 268−279.
32. Chirita, C. N., Necula, M., and Kuret, J. (2004) Ligand-dependent inhibition and reversal of tau filament formation, *Biochemistry 43*, 2879−2887.
33. Pickhardt, M., Gazova, Z., von Bergen, M., Khlistunova, I., Wang, Y., Hascher, A., Mandelkow, E. M., Biernat, J., and Mandelkow, E. (2005) Anthraquinones inhibit tau aggregation and dissolve Alzheimer's paired helical filaments in vitro and in cells, *J. Biol. Chem. 280*, 3628−3635.
34. Taniguchi, S., Suzuki, N., Masuda, M., Hisanaga, S., Iwatsubo, T., Goedert, M., and Hasegawa, M. (2005) Inhibition of heparin-induced tau filament formation by phenothiazines, polyphenols, and porphyrins, *J. Biol. Chem. 280*, 7614−7623.
35. Necula, M., Chirita, C. N., and Kuret, J. (2005) Cyanine dye N744 inhibits tau fibrillization by blocking filament extension: implications for the treatment of tauopathic neurodegenerative diseases, *Biochemistry 44*, 10227−10237.
36. Brandt, R., Hundelt, M., and Shahani, N. (2005) Tau alteration and neuronal degeneration in tauopathies: mechanisms and models, *Biochim. Biophys. Acta 1739*, 331−354.
37. Dinoto, L., Deture, M. A., and Purich, D. L. (2005) Structural insights into Alzheimer filament assembly pathways based on site-directed mutagenesis and S-glutathionylation of three-repeat neuronal Tau protein, *Microsc. Res. Tech. 67*, 156−163.
38. Eliezer, D., Barre, P., Kobaslija, M., Chan, D., Li, X., and Heend, L. (2005) Residual structure in the repeat domain of tau: echoes of microtubule binding and paired helical filament formation, *Biochemistry 44*, 1026−1036.
39. Rankin, C. A., Sun, Q., and Gamblin, T. C. (2005) Pseudophosphorylation of tau at Ser202 and Thr205 affects tau filament formation, *Brain Res. Mol. Brain Res. 138*, 84−93.
40. Spillantini, M. G., Murrell, J. R., Goedert, M., Farlow, M. R., Klug, A., and Ghetti, B. (1998) Mutation in the tau gene in familial multiple system tauopathy with presenile dementia, *Proc. Natl. Acad. Sci. U.S.A. 95*, 7737−7741.
41. Hutton, M., Lendon, C. L., Rizzu, P., Baker, M., Froelich, S., Houlden, H., Pickering-Brown, S., Chakraverty, S., Isaacs, A., Grover, A., Hackett, J., Adamson, J., Lincoln, S., Dickson, D., Davies, P., Petersen, R. C., Stevens, M., de Graaff, E., Wauters, E., van Baren, J., Hillebrand, M., Joosse, M., Kwon, J. M., Nowotny, P., Che, L. K., Norton, J., Morris, J., Reed, L., Trojanowski, J., Basun, H., Lannfelt, H., Neystat, M., Fahn, S., Dark, F., Tannenberg, T., Dodd, P., Hayward, N., Kwok, J., Schofield, P., Andreadis, A., Snowden, J., van Swieten, J., Mann, D., Lynch, T., and Heutink, P. (1998) Association of missense and 5′-splice-site mutations in tau with the inherited dementia FTDP-17, *Nature 393*, 702−705.
42. Clark, L. N., Poorkaj, P., Wszolek, Z., Geschwind, D. H., Nasreddine, Z. S., Miller, B., Li, D., Payami, H., Awert, F., Markopoulou, K., Andreadis, A., D'Souza, I., Lee, V. M. Y., Reed, L., Trojanowski, J. Q., Zhukareva, V., Bird, T., Schellenberg, G., and Wilhelmsen, K. C. (1998) Pathogenic implications of mutations in the tau gene in pallido-ponto-nigral degeneration and related neurodegenerative disorders linked to chromosome 17, *Proc. Natl. Acad. Sci. U.S.A. 95*, 13103−13107.
43. Mukrasch, M. D., Biernat, J., von Bergen, M., Griesinger, C., Mandelkow, E., and Zweckstetter, M. (2004) *J. Biol. Chem. 280*, 24978−24986.

44. Tomoo, K., Yao, T.-M., Minoura, K., Hiraoka, S., Sumida, M., Taniguchi, T., and Ishida, T. (2005) Possible role of each repeat structure of the microtubule-binding domain of the tau protein in in vitro aggregation, *J. Biochem. 138*, 413−423.
45. Goux, W. J., Kopplin, L., Nguyen, A. D., Leak, K., Rutkofsky, M., Shanmuganandam, V. D., Sharma, D., Inouye, H., and Kirschner, D. A. (2004) The formation of straight and twisted filaments from short tau peptides, *J. Biol. Chem. 279*, 26868−26875.
46. Li, L., von Bergen, M., Mandelkow, E. M., and Mandelkow, E. (2002) Structure, stability, and aggregation of paired helical filaments from tau protein and FTDP-17 mutants probed by tryptophan scanning mutagenesis, *J. Biol. Chem. 277*, 41390−41400.
47. Ramachandran, R., Tweten, R. K., and Johnson, A. E. (2004) Membrane-dependent conformational changes initiate cholesterol-dependent cytolysin oligomerization and intersubunit beta-strand alignment, *Nat. Struct. Mol. Biol. 11*, 697−705.
48. Inouye, H., Sharma, D., Goux, W. J., and Kirschner, D. A. (2006) Structure of core domain of fibril-forming PHF/Tau fragments, *Biophys. J. 90*, 1774−1789.
49. Arrasate, M., Perez, M., Armas-Portela, R., and Avila, J. (1999) Polymerization of tau peptides into fibrillar structures. The effect of FTDP-17 mutations, *FEBS Lett. 446*, 199−202.
50. Nacharaju, P., Lewis, J., Easson, C., Yen, S., Hackett, J., Hutton, M., and Yen, S. H. (1999) Accelerated filament formation from tau protein with specific FTDP-17 missense mutations, *FEBS Lett. 447*, 195−199.
51. Goedert, M., Jakes, R., and Crowther, R. A. (1999) Effects of frontotemporal dementia FTDP-17 mutations on heparin-induced assembly of tau filaments, *FEBS Lett. 450*, 306−311.
52. Gamblin, T. C., King, M. E., Dawson, H., Vitek, M. P., Kuret, J., Berry, R. W., and Binder, L. I. (2000) In vitro polymerization of tau protein monitored by laser light scattering: method and application to the study of FTDP-17 mutants, *Biochemistry 39*, 6136−6144.
53. Rizzini, C., Goedert, M., Hodges, J. R., Smith, M. J., Jakes, R., Hills, R., Xuereb, J. H., Crowther, R. A., and Spillantini, M. G. (2000) Tau gene mutation K257T causes a tauopathy similar to Pick's disease, *J. Neuropathol. Exp. Neurol. 59*, 990−1001.
54. Fernandez-Escamilla, A.-M., Rousseau, F., Schymkowitz, J., and Serrano, L. (2004) Prediction of sequence-dependent and mutational effects on the aggregation of peptides and proteins, *Nat. Biotechnol. 22*, 1302−1306.
55. Fraser, P. E., McLachlan, D. R., Surewicz, W. K., Mizzen, C. A., Snow, A. D., Nguyen, J. T., and Kirschner, D. A. (1994) Conformation and fibrillogenesis of Alzheimer Aβ peptides with selected substitution of charged residues, *J. Mol. Biol. 244*, 64−73.
56. Permanne, B., Adessi, C., Fraga, S., Frossard, M.-J., Saborio, G. P., and Soto, C. (2002) Are beta-sheet breaker peptides dissolving the therapeutic problem of Alzheimer's disease?, *J. Neural. Transm., Suppl. 62*, 293−301.
57. Adessi, C., Frossard, M.-J., Boissard, C. Fraga, S., Bieler, S., Ruckle, T., Vilbois, F., Robinson, S. M., Mutter, M., Banks, W. A., and Soto, C. (2003) Pharmacological profiles of peptide drug candidates for the treatment of Alzheimer's disease, *J. Biol. Chem. 278*, 13905−13911.
58. Soto, C., Saborio, G. P., and Permanne, B. (2000) Inhibiting the conversion of soluble amyloid-beta peptide into abnormally folded amyloidogenic intermediates: relevance for Alzheimer's disease therapy, *Acta Neurol. Scand., Suppl. 176*, 90−95.
59. Sigurdsson, E. M., Permanne, B., Soto, C., Wisniewski, T., and Frangione, B. (2000) In vivo reversal of amyloid-beta lesions in rat brain, *J. Neuropathol. Exp. Neurol. 59*, 11−17.
60. Soto, C., Kindy, M. S., Baumann, M., and Frangione, B. (1996) Inhibition of Alzheimer's amyloidosis by peptides that prevent beta-sheet conformation, *Biochem. Biophys. Res. Commun. 226*, 672−680.
61. Soto, C., Sigurdsson, E. M., Morelli, L., Kumar, R. A., Castano, E. M., and Frangione, B. (1998) Beta-sheet breaker peptides inhibit fibrillogenesis in a rat brain model of amyloidosis: implications for Alzheimer's therapy, *Nat. Med. 4*, 822−826.
62. Soto, C., Kascsak, R. J., Saborio, G. P., Aucouturier, P., Wisniewski, T., Prelli, F., Kascsak, R., Mendez, E., Harris, D. A., Ironside, J., Tagliavini, F., Carp, R. I., and Frangione, B. (2000) Reversion of prion protein conformational changes by synthetic beta-sheet breaker peptides, *Lancet 355*, 192−197.

BI061422+